Special Issue Papers

Echography Using Correlation Techniques: Choice of Coding Signal

Mohamed A. Benkhelifa, Marcel Gindre, *Member, IEEE,* Jean-Yves Le Huerou, and Wladimir Urbach

***Abstract*—Theoretical studis made in the early 1980's suggest that ultrasonic imaging using correlation technique can overcome some of the drawbacks of classical pulse echography. Indeed by transmitting a continuous coded signal and then compressing it into a short, high resolution pulse at the receiver the total signal to noise ratio (SNR) is improved. The target location is determined by cross correlation of the emitted and the received signal. The band compression allows, by increasing SNR, the retrieval of echo signals buried in the receiver noise. Thus in medical-type echography, where the signal attenuation at fixed depth is proportional to the frequency, the SNR improvement allows the use of higher frequency signals and leads to improved resolution. We report here the results of comparative experimental studies of simple echo B type images as obtained by the classical pulse echo and correlation techniques. Because the optimisation of the coded signal plays a crucial role in the performance of the correlation technique we will also present a comparative study of the performances of the most common codes (m-sequences and complementary series). In particular we shall emphasise the following points:**

- **the relative importance of the central lobe as compared to the side lobes of the correlation function, which is directly related to the dynamic of the imaging system,**
- **the width of the correlation peak which is directly related to the axial resolution of the system,**
- **the facility of the realisation.**

The merit of B-mode images obtained with the coded signals will be discussed showing that as far as signal modulation is used the best results are obtained with periodic m-sequences.

I. Introduction

PULSE echo reflection techniques have been used for ultrasonic boundary location in most commercial non-destructive testing instruments and in diagnostic medicine for several decades. These real time ultrasonic systems are often limited in average transmitted power by peak power constraints even in highly attenuating propagation media. In the case of medical ultrasound devices, for example, the peak power limit arises from the risk of causing tissue damage rather than from signal emission limits of the instrument. Obviously the energy in the reflected signal depends on the transmitted energy, so the signal to noise ratio (SNR) limit, or penetration depth, is also determined by this factor. In stationary media signal averaging leads to SNR enhancement but is time consuming. Coded excitation in correlation based systems [1] permits a dramatic improvement of SNR at modest peak levels as compared to conventional pulsed techniques. In this systems the target location is determined by cross correlation of the emitted and of the received noisy signal. It has been shown that in some cases correlation can provide a theoretically unlimited signal to noise ratio enhancement [2] which is defined as the ratio of the SNR at correlation output to that at the receiver prior to correlation.

This paper attempts specifically to address the problem of choice of the appropriate coding sequence. In order to ensure that all coding sequences have the same resolution, we consider only sequences which are made of elementary pulses of equal duration. In addition, the total energy launched into the propagation medium will be the same for all sequences. In the following different types of large bandwidth transmitted signals are discussed and their merits (in terms of resolution, SNR, and its variation in the presence of moving targets) are presented. Afterwards, the simulation of the propagation in a real medium of the most promising coded signals is presented. Finally, a prototype of an imaging system is described and the advantage of modulated m-sequences over modulated complementary series is demonstrated.

Manuscript received June 8, 1993, revised January 27, 1994; accepted April 3, 1994. This project was supported by ARC Grant 6174, ANVAR Grant A87069QAC, and with funds from INSERM No. 88-90-10.

The authors are with the Laboratoire d'Imagerie Paramétrique URA CNRS 1458, 75006 Paris, France.

IEEE Log Number 9403348.

II. Background

An ultrasonic transmit-receive system based on classical echography as well as on correlation may be represented as shown in Fig. 1, where $e(t)$ and $s(t)$ are, respectively, the emitted and the received signal, and $h(t)$ is the global transmit-receive impulse response of the transducers and the propagating medium.

In the linear regime of operation it follows from classical signal theory that

$$s(t) = \int_{-\infty}^{\infty} h(u)e(t-u)\,du = e(t) * h(t). \qquad (1)$$

If $e(t) \approx \delta(t)$ where $\delta(t)$ is the Dirac distribution, then $s(t) \approx h(t)$. Thus in classical "idealized" echography the impulse response $h(t)$ is obtained directly. In practice, $e(t)$

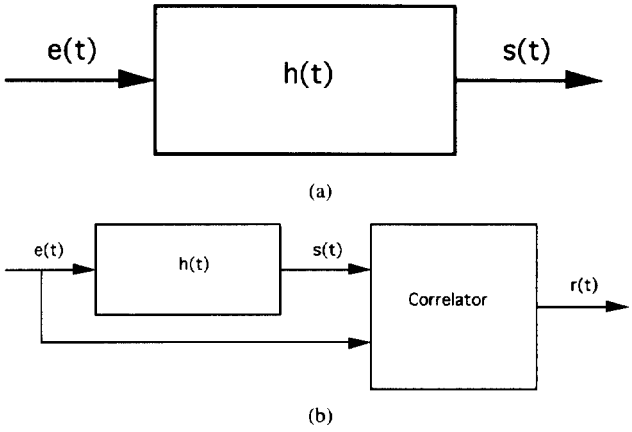

Fig. 1. Schematic block diagram of the ultrasonic imaging system. (a) Classical system. (b) System using correlation techniques.

is a high voltage pulse. Its duration is short in order to fully exploit the bandwidth of the transducer and to maximise the resolution.

There is a second method for evaluating $h(t)$ [3]. In correlation based systems the output is

$$r(t) = \int_{-\infty}^{\infty} s(\xi)e(\xi - t)\,d\xi = \Gamma_{ee}(t) * h(t) \tag{2}$$

where $\Gamma_{ee}(t)$ is the autocorrelation function of the emitted signal $e(t)$.

If $e(t)$ is such that $\Gamma_{ee}(t) \approx \delta(t)$, we have $r(t) \approx h(t)$. In other words, this means that if we choose an emitting signal such that its autocorrelation function is a Dirac distribution, the impulse response of the system is given by the cross-correlation function between emission and reception.

Only white noise gives an autocorrelation function which is equivalent to a Dirac distribution. Several other types of transmitted signals have been proposed by different authors. These include wide-band m -sequences [4]–[6], random noise [1], chirp [7]–[9], Golay codes [10], [11], Barker code [12]. The autocorrelation functions of such signals consist of a main peak and secondary maxima. The higher the value of the ratio of main peak amplitude (Lp) to the highest secondary lobe amplitude (Ls), the closer will be the shape of Γ_{ee} to the Dirac function. For chirp codes Lp/Ls is only equal to 13 dB. In order to improve this value a very efficient apodization is necessary which leads to a broadening of Γ_{ee} and thus to a significant decrease of axial resolution [13]. It has been shown recently that by using an adapted signal processing the Lp/Ls ratio can reach 40 dB [9]. In the next section we shall briefly review discrete codes which fit the best to our purpose.

III. Evaluation of Coded Signals

A variety of codes are available for application in the system. Factors affecting the choice of code are: ease in generation: peak to side lobe ratio (Lp/Ls) in the correlation function, and the processing complexity. With a microcomputer system, generation of any code can easily be done by writing the appropriate data to the transmission buffer in the code generation unit. Software processing for various codes is straightforward. Thus the main criterion is the value of peak to side lobe ratio (Lp/Ls). In order to allow easy comparison between the most common codes we will present hereafter a comparative study based on the following protocol. 1) For each code the number and/or the amplitude of its binary elements can vary. However the total energy launched into the propagating medium is the same for all codes considered. For a fixed amplitude of any code this requires that the product of the emission time and the square of the amplitude be constant. 2) In order to make the axial resolution of all codes equivalent, the duration of each binary element of any code was fixed at the same value τ. 3) All simulations were made with sampled signals. For any code the number of samples per binary element was 16. 4) In the correlation system the returning wave form from a moving target no longer matches the reference signal. In order to determine the mismatch effects we shall consider the variation of Lp/Ls with the Doppler shift frequency.

Let

$$e_{\mathrm{mod}}(t) = \sum_{n=1}^{N} a_n \Pi_n(t) \exp\left[i(\omega_0 t + \varphi_n)\right] \tag{3}$$

be the general expression of the modulated and coded signal where a_n is the amplitude of the nth binary element of duration τ, and φ_n is the corresponding phase, N is the number of binary elements ($N\tau = T$) and

$$\Pi_n(t) = \begin{cases} 1 & \text{for } (n-1)\tau \le t \le n\tau \\ 0 & \text{elsewhere} \end{cases}. \tag{4}$$

We shall consider three different types of code:

$$\mathrm{A} : a_n = 1 \text{ and } \varphi_n = 0 \text{ or } \pi$$
$$\mathrm{B} : a_n = 1 \text{ and } \varphi_n \text{ variable}$$
$$\mathrm{C} : a_n \text{ and } \varphi_n \text{ variable}.$$

For codes of type A the autocorrelation function is given for the periodic case by:

$$\Gamma_{ee}(k) = \sum_{m=1}^{N} e_j e_m \tag{5}$$

with $k \ge 0$ and $j = (m + k)$ modulo N, and for nonperiodic case, and by:

$$\Gamma_{ee}(k) = \sum_{m=1}^{N-k} e_j e_m \tag{6}$$

with $k \ge 0$ and $j = m + k$. For codes of types B or C we have calculated the autocorrelation function following the method suggested by Bernfeld and Liebman [14].

A-Type Codes

For Barker's codes [15] the ratio $(Lp/Ls)_{\max}$ is about 22 dB. This result can be improved by combined Barker's codes [16], [17] but it is limited to a value of 30 dB. For our purpose the m-sequence and complementary Golay codes are better candidates.

Maximal Length Sequence: The m-sequence [18], simpler to implement, is a perfectly deterministic sequence of $N = (2n - 1)$ binary digits which displays a certain number of properties of randomness approximating those of white noise. It is often referred to as a pseudorandom binary sequence or pseudonoise. In the case of nonperiodic emission of an N element sequence [19], the peak to side lobe ratio $Lp/Ls \leq 20 \log \sqrt{N}$. The ratio $Lp/Ls = 20 \log N$ is equal to 42 dB for $N = 127$ when the m-sequence is transmitted continuously. This precludes however the use of a single transducer, which is not the case with Golay's codes.

Golay's Codes: Golay's codes are pairs of complementary binary codes [20]. The autocorrelation function of each code in a pair has a central peak and a range of side lobes of identical shape but of opposite sign. The addition of the autocorrelation functions from a pair of complementary codes produces a large triangular central peak with no side lobes ($Lp/Ls \rightarrow \infty$). The length of Golay's code usable by any correlation system is only limited by the generation capability of the system. Other codes have also been shown to have the same zero range side lobe property [21]–[23]. It is worth noting that because Golay's codes involve the sequential transmission of two related sequences, real time imaging of some systems is prohibited with this type of code.

B-Type Codes

Type B codes were generated as suggested by Frank [24]. Consider a code of N elements. Let j and m be two indexes with $0 \leq j \leq \sqrt{N}$ and $0 \leq m \leq \sqrt{N}$. The phase of each element $\varphi_{jm} = [2\pi/\sqrt{N}](j + m)$. The N elements of code are thus emitted in $\sqrt{N}$ subgroups. For each subgroup j is kept fitted while m runs from 0 to $\sqrt{N} - 1$. For sufficiently high values of N one can show [25] that

$$\frac{Lp}{Ls} = 20 \log (\pi \sqrt{N}). \tag{7}$$

For $Lp/Ls \sim 50$ dB, the phase is in units of $2\pi/\sqrt{N} \approx 3.6°$. This is hard to implement when the operating frequency is of the order of some Megahertz. That is why codes with only two phase values are more practical and appear more attractive.

C-Type Codes

Huffman has shown [26]–[28] that by varying the amplitude and the phase of each element of the coding sequence it is possible to increase significantly the peak to side lobe ratio. In spite of very promising results, however, implementation of Huffman coding sequences remains very delicate. Kretschmer and Lin [29] have shown that an error of 5% in the form of each of 64 binary elements of a Huffman sequence induces a loss of 20 dB in the peak to noise ratio. Such sensitivity makes it impractical to use.

It is apparent from previous discussion that only m-sequence and Golay's codes provide sufficient SNR and easy implementation to ultrasonic imaging. In the following we shall only consider this two types of codes and the corresponding SNR degradation due to Doppler effects.

IV. Moving Target Effects

In case of a multifrequency broadband waveform, the effect of a moving target can be described as a modification of the duration of the waveform which is proportional to the target velocity. In classical echographic techniques the result is a longer or shorter burst. In a correlation system the motion of the target will produce a cross-correlation function which will not align as required for optimum cancellation of lateral lobes. Thus the Doppler shift should produce a significant degradation of the peak to sidelobe ratio mainly due to an increase in amplitude of the lateral lobes. To determine the effects of the mismatch of wide-band signals, one can analyze the form of the ambiguity function [3], [30]. $\chi(\theta, \omega_d) = \int a^*(t)a(t - \theta) \exp(i\omega_d t)\, dt$. Where $\omega_d = 2\pi f_d$ is the pulsation shift produced by the Doppler effect. When $\omega_d = 0, \chi(\theta)$ is simply the autocorrelation function of the complex envelop $a(t)$ of the emitted signal $e(t)$. Using the expression for χ, the modulus of the ambiguity functions were then plotted for m-sequences and Golay codes [31]. The χ functions were defined in terms of the delay (τ axis) and a dimensionless parameter $T \cdot f_d$ where T is the duration of the coded sequence and f_d is the Doppler shift.

For a periodic m-sequence of 127 binary elements the ambiguity function is plotted in Fig. 2. For zero Doppler shift $(f_d = 0) Lp/Ls \approx 42$ dB as expected. When f_d increases, the secondary lobes rise very rapidly, and the peak to side lobe ratio reaches the value of 23 dB for $T \cdot f_d = 0.2$.

The Golay's codes are emitted in a consecutive manner, and it is probably optimistic to assume that the Doppler shift is exactly the same for both sequences. However, if this hypothesis is correct, the resulting ambiguity function χ is shown in Fig. 3. To allow better readability χ was truncated at -60 dB, although the Lp/Ls value for $fd = 0$ is theoretically infinite. Here again, the amplitude of the secondary lobes increases rapidly with f_d, and for $T \cdot f_d = 0.2$, Lp/Ls reaches 25 dB, a slightly better value than in the case of the m-sequence. This requires two sequences of 128 b each, however, doubling the energy launched into the medium.

Both codes are sensitive to Doppler shifts. However they can, in principle, easily provide a 50 dB peak to noise ratio. Periodic m-sequences are easy to generate, but because of continuous emission the need to use separate transducers for transmission and reception seems to be one potential drawback of the method. Golay's codes offer the advantage of side lobe cancellation and seem more promising at this stage of study where the propagating medium is absent. To understand in what manner the propagating medium can influence our results, we shall consider the propagation of Golay codes and m-sequences through a simulated medium in the next part of this paper.

V. Simulated Results

The m-sequences and complementary series were extensively used by several authors [5], [11], [31], [32]. However, even if the theoretical improvement of the SNR is obvious, the observed SNR is far from the theoretical prediction, especially

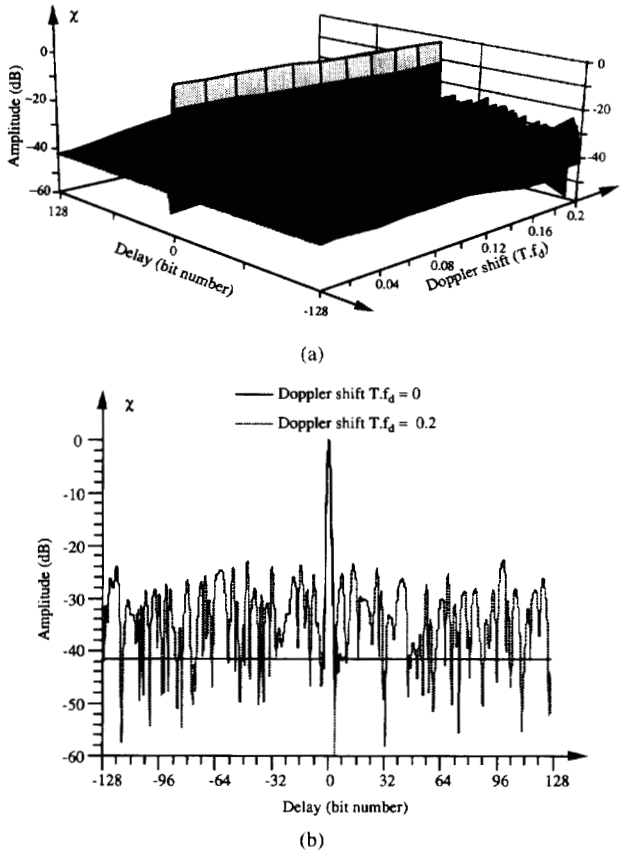

Fig. 2. Ambiguity function for a 127 bit m-sequence. (a)3-D representation. (b) Correlation function for fixed Doppler shift.

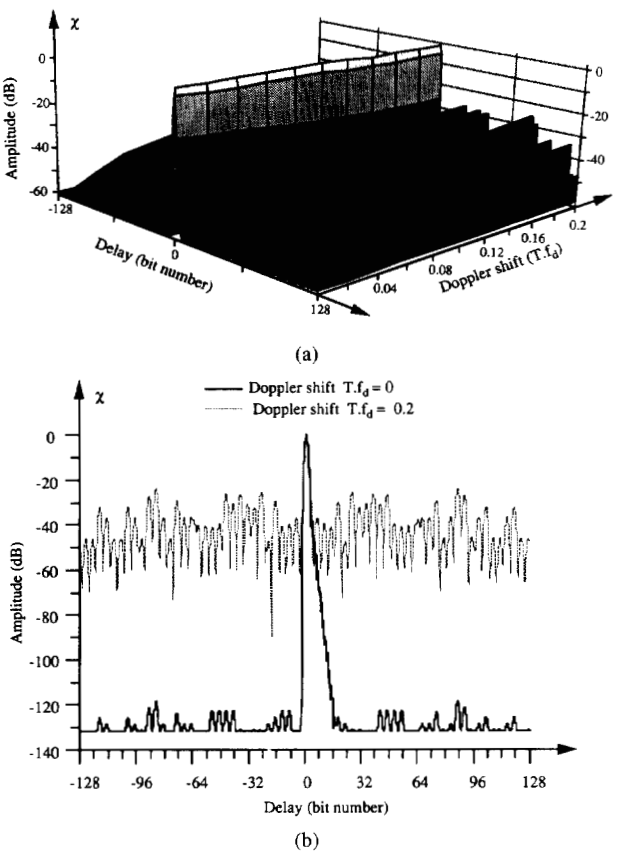

Fig. 3. Ambiguity function for a 128 bit Golay's code. (a) 3-D representation. (b) Correlation function for fixed Doppler shift.

when Golay series are used. This could be due, as we shall see, to at least two different factors.

We have simulated the propagation of coded sequences using software developed in our laboratory. The software allows us to simulate the four fundamental steps: signal modulation, transmission, reception, and signal processing. The signal is phase modulated in order to place its frequency bandwidth at that of the transducer. This ensures maximum energy transfer. We use phase shift keying (PSK) modulation, i.e., $\varphi_n = 0$ or $\varphi_n = \pi$ in (3) and $a_n = 1$. The spectral density of the emitted signal prior to modulation is

$$E(f) = N\tau^2 \left[\frac{\sin(\pi f \tau)}{\pi f \tau}\right]^2 \tag{8}$$

and

$$E_{\text{mod}}(f) = \frac{1}{2}[E(f+f_0) + E(f-f_0)] \tag{9}$$

after modulation. The transmission model accounts for the transducer and the propagating medium. From the classical signal theory:

$$s(t) = e(t) * h_{er}(t) * h_{re}(t) * h_a(M,t) * h_d(M,t) \tag{10}$$

where

- $d/2$ is the distance from transducer to the target position M
- $h_{er}(t) = h_{re}(t)$ are the impulse response, operating in the emitted and receiving modes, of the transducer modelled by a Gaussian band-pass filter:

$$H_{er}(f) = H_{re}(f) = \exp\left(\frac{-(f-f_0)^2}{B^2}\right) \tag{11}$$

where B is the bandwidth of the transducer.

- $h_a(M,t)$ is the impulse response of the propagating medium due to the attuenuation coefficient β. Following Kuc [33] we have:

$$|H_a(f)| = \exp(-\beta f d) \tag{12}$$

with

$$\arg(H_a(\omega)) = \frac{1}{2\pi} VP \cdot \left[\int_{-\pi}^{+\pi} \ln|H_a(\nu)| \operatorname{cotg}\left(\frac{\nu-\omega}{2}\right) d\nu\right] \tag{13}$$

where VP is the Cauchy principal value [34] and $\omega = 2\pi f/f_e$ with f_e is sampling frequency (in our case $f_e = 100$ MHz).

- $h_d(M,t)$ is the impulse response due to diffraction. It accounts for the finite dimension of the transducer. It can be shown that diffraction effects are similar to those of a low-pass filter with attenuation increasing with the distance from the transducer [35]:

$$H_d(f) = c^2 \Delta t^2 \operatorname{sinc}^2[f\Delta t] e^{-4i\pi f(t-(\Delta t/2))} \tag{14}$$

where sinc $x = \sin \pi x / \pi x$, c is the sound velocity, and Δt is the delay between the signals arriving at the target from the most distant and the nearest parts of the transducer.

The receiver part has in phase and quadrature phase channels. After the demodulation, low-pass filtering is made by a Butterworth type filter [36]. Its transfer function is

$$|F(\omega)|^2 = \left(1 + \left(\frac{\omega}{\omega_c}\right)^{2n}\right)^{-1} \tag{15}$$

where the cutoff frequency $f_c = \omega_c / 2\pi$, and the order of the filter n can be chosen as needed. After low-pass filtering, the output from each channel is translated into the frequency domain using the Cooley-Tukey fast Fourier transform (FFT) algorithm [37], [38]. The resulting spectrum is then multiplied by the spectrum of the emitted signal $E(f)$, and the result is transformed back to time domain. The corresponding outputs are then squared and added. The result is the cross-correlation peak whose location corresponds to the distance between the target and the transducer. In other words:

$$\Gamma^2(t) = \Gamma_1^2(t) + \Gamma_2^2(t) \tag{16}$$

$$\Gamma^2(t) = \{\mathcal{F}^{-1}[S_1(f)E(f)]\}^2 + \{\mathcal{F}^{-1}[S_2(t)E(f)]\}^2 \tag{17}$$

where $S_1(f)$ and $S_2(f)$ are the Fourier transforms of the two received demodulated and filtered signals.

Simulations where conducted with m-sequences and Golay codes. The m-sequences employed were 1023 b long while Golay codes had 1024 b each. The same energy was launched into the medium by each emitted m-sequence and by each one of the two complementary series. The central frequency of the transducer is $f_0 = 6.25$ MHz and its diameter $2r = 8$ mm. In order to optimize the resolution, the bit duration, τ, is equal to $1/f_0 = 160$ ns. With the sound velocity $c = 1530\,\mathrm{ms}^{-1}$, the corresponding sound wavelength is $\lambda = cf_0^{-1} = 0.24$ mm, and the limit Fresnel Fraunhofer zone [39] $z_F = r^2\lambda^{-1} \approx 65.4$ mm. In order to avoid memory overflow and to achieve reasonable computation times, simulations were made over distances of 125 mm with maximal scattering density equal to $3/\lambda$.

The first simulations were conducted with only one target placed at the distance of 80 mm from the transducer and with an infinite transducer's bandwidth. In order to allow easy comparison of result, the output signal was normalized to 0 dB. For complementary series the noise level observed in Fig. 3 is due to round-off error in FFT computing, and the SNR value is still greater than 120 dB. For m-sequences when a discrete Fourier transform algorithm is used, the expected SNR value of 60 dB (with $N = 1023$ b) is achieved. The diffraction filter effects are clearly observed in Fig. 4, where the peak amplitude decreases with the increasing dimensionless parameter Z

$$Z = \frac{\text{target to transducer distance}}{\text{transducer radius } r} \tag{18}$$

and where the width variation of the correlation peak was also plotted for m-sequences and for Golay codes. When the attenuation effects are added the peak amplitude decreases

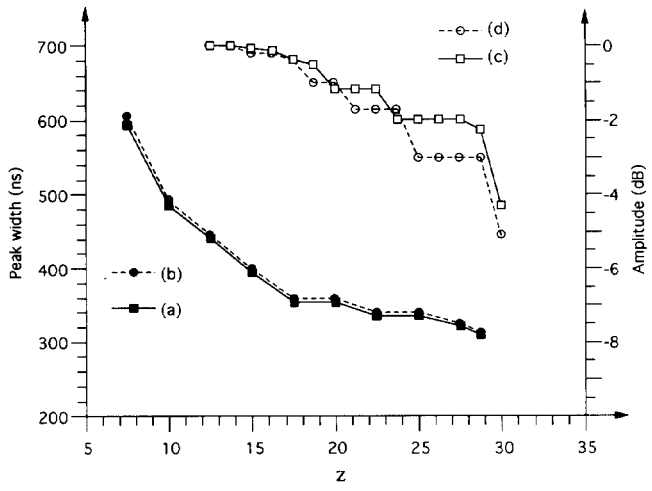

Fig. 4. Diffraction filter effects. Variation of the peak amplitude (c, d) and variation of the peak width at −20 dB (a, b) versus the normalized distance Z for m-sequence (continuous lines) and Golay's codes (dotted lines).

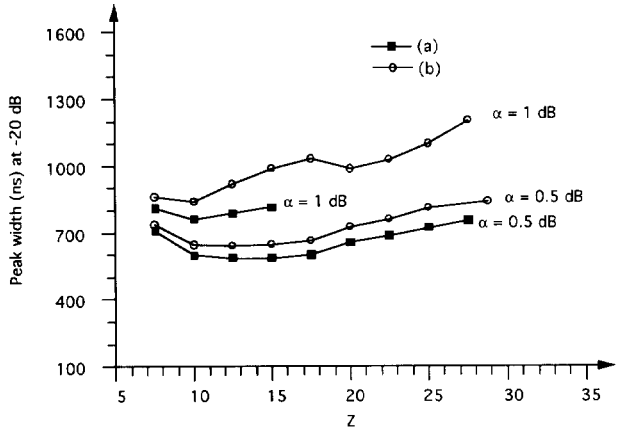

Fig. 5. Same as Fig. 4 but the effects of attenuation are added ($\alpha = 0.5$ dB or 1 dB) (a) 1023 bit m-sequence; (b) two 1024 bit Golay's codes.

exponentially with Z. The increase of the width of the correlation peak with Z due to rapid attenuation of high frequency components in the emitted signal is shown in Fig. 5. At low Z values the principal effect is due to diffraction and peak width decreases. At higher Z values the observed variations are due to the attenuation itself. The influence of the transducer, which is often modeled as a Gaussian type band-pass filter, is well known and will be omitted here.

At this point we wish to emphasize a dramatic decrease of SNR observed when the modulation-demodulation process is not carefully simulated. Both codes, the m-sequences and the complementary series, are modulated using PSK coherent modulation.

The use of complementary series implies the emission of two complementary sequences. A small displacement Δd of the target between two emissions corresponds to the phase

$$\Delta\phi = \frac{2\pi\Delta d}{\lambda} \tag{19}$$

which leads to SNR degradation as shown in Fig. 6. For medical imaging where the movements are slow the $\Delta\phi$ variation is negligible. Furthermore the suppression of the continuous component by electronic circuits leads to further degradation

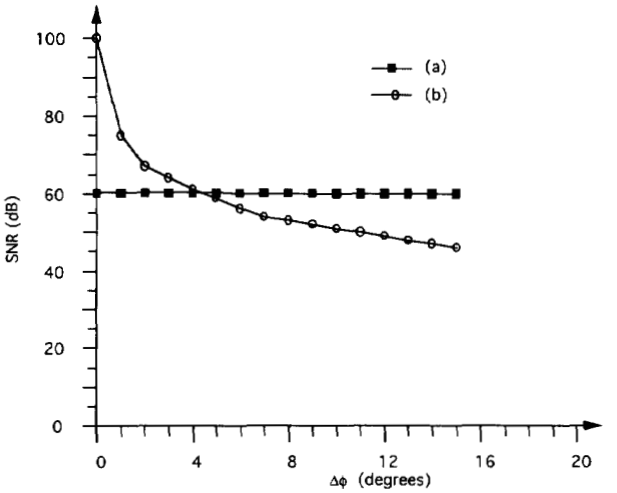

Fig. 6. SNR degradation versus phase error $\Delta\phi$ between two 1024 bit Golay's codes. A variation of 10° in $\Delta\phi$ induces a SNR of 40 dB (this corresponds to $\Delta d = \frac{\lambda\Delta\phi}{2\pi} = 120\,\mu$m.

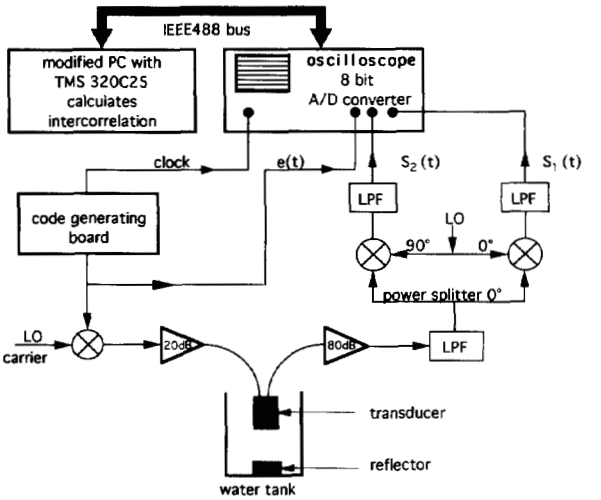

Fig. 7. Schematic representation of the digital correlation system assembled in our laboratory. LO: Local oscillator, LPF: Low-pass filter, $e(t)$, $S_1(t)$ and $S_2(t)$ are, respectively, the reference code, the two received signals applied to the correlator.

in Lp/Ls ratio. For the Golay sequence of length $N = 2^{2p}$, the difference between the number of bits of value $+1$ and the value -1 is $\Delta n = 2^p$. The non nil Δn value leads to a continuous component in a coding sequence. Its suppression by demodulation creates an asymmetric code ($U_+ \neq U_-$) and the secondary lobes of correlation function are no longer fully compensated. The resulting SNR $\leq 20\log(\Delta n/N)$ is equal to 30 dB for $N = 1024$.

For these reasons we believe that the use of the complementary series in acoustical imaging is inadequate, as far as modulation is used. An other possibility is to use direct sequencing. In this case however much of signal is outside of the transducer's bandwidth and is wasted [40].

VI. Experimental Results

A-Type Images

The digital correlation system assembled in our laboratory is shown in Fig. 7. To sum self correlation functions from two complementary codes, two 1024 bits codes were transmitted and correlated in sequential mode, whereas with 1023 bit length m-sequences the system operates in cyclic mode.

To perform the continuous (cyclic) correlation we used a concave annular array. The concave transducer improves spatial resolution, and the eventual use of electronically focused annular phased arrays should allow us to vary the transducer's focal length around the geometrical preselected length of 10 cm. In the first experiments, reported here after, the central part of the transducer (diameter $\approx$1.4 cm) is used as an emitter, while the nearest of equiarea annuli is operated in receiver mode. The central frequency is $f_T = 7.5$ MHz, and its –3 dB bandwidth $B = 2$ MHz. In this configuration the lateral resolution is rather poor ($\pm$0.4 mm at -6 dB). Nevertheless it still allows an interesting comparison between the classical echography and correlation, especially in A-mode where the lateral resolution is unimportant. For maximum transmitted energy a phase shift keying (PSK) modulation was chosen. The binary code was phase modulated to the center frequency of the transducer. For a good resolution the duration of each bit of the coding sequence should be as a short as possible. However, due to our transducer's bandwidth when the pulse duration is $t \leq 0.28$ ms, more than 10% of the incoming energy is wasted. In the receiving unit the local carrier is derived from the same source as the transmitted carrier so that synchronous detection can be achieved. The return echoes are split into two channels and demodulated by the same functions used for initial modulation but separated from one another by 90° in phase. The outputs, $S_1(t)$ and $S_2(t)$, from the two channels are correlated with delayed replicas of the transmitted sequence, $e(t)$. The correlated results are squared and added, and the final result is displayed on the screen. The correlation is done in software on the microcomputer while a digital scope with 8 bit resolution serves as the data acquisition unit.

In Fig. 8 we present A-scan results obtained with a small tip of a rod (13 mm high and 0.2 mm diameter) placed in the front of the large reflector. The echo from the tip is designated by 1, the echo from the front plane of the large reflector by 2 and its rear plane by 3. In the classical pulse-echo mode $e(t)$ is a 150 V pulse. With the coded signals $e(t)$ had an amplitude of 1 V. Both codes emitted at the frequency $f_c = \tau^{-1} =$ 1.875 MHz. Since we have checked that SNR is fairly constant for $2f_c \leq f_s \leq 8f_c$, we used $f_s = 4.0f_c = 7.5$ MHz for convenience. The classical echo A signal is shown in Fig. 8(a). The SNR is about 20 dB due to the relatively low sensitivity of our transducer, which lacks time gain control.

When $e(t)$ is an m-sequence, one obtains the correlated signal shown in Fig. 8(b). Here the SNR is nearly equal to 50 dB instead of the expected theoretical value of 60 dB obtained for the transducer's bandwidth B = ∞. Indeed, it is well known that if $E(f)$ is the spectral density of emitted signal $e(t)$, the signal energy is simply $W = \int E(f)\,df$ and the energy transmitted to the medium by a transducer modelled by a Gaussian filter is

$$W_T = \int E(f)\exp\left\{-\left[\frac{f-f_0}{B}\right]^2\right\}df \qquad (20)$$

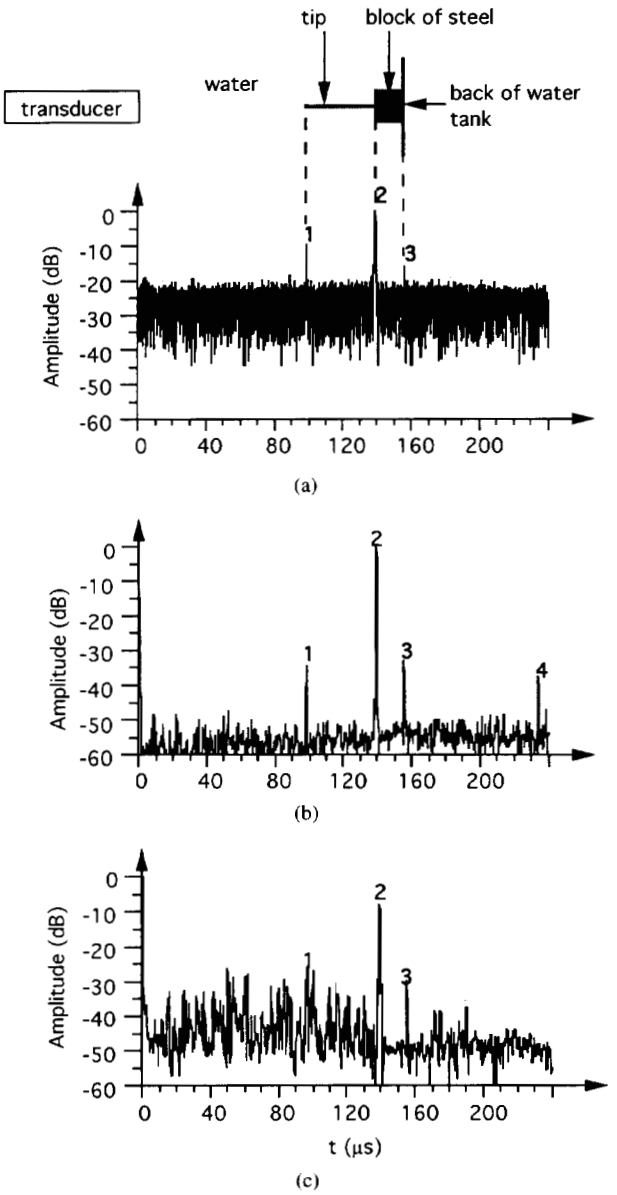

Fig. 8. The object and the corresponding echograms as obtained with (a) classical pulse method, (b) m-sequence, (c) complementary series.

Thus the attenuation of the correlation peak is $10 \log [W_T/W]$, whereas the noise, mainly due to the electronics, remains constant. With $f_0 = 7.5$ MHz and $B \approx 2$ MHz this leads to a decrease in the central peak of 6 dB.

As expected (see the end of Section V) for Golay codes SNR $\approx$ 30 dB [Fig. 8(c)]. Obviously, the m-sequences evidently lead to the best results.

B-Type Images

With the same very broad ultrasonic beam we obtained some preliminary B type images of a very simple object: a hole 3 mm in diameter and 10 mm in depth was drilled in the center of a cylindrical block of duraluminum. The transducer was moved along a diameter, and the resulting B echogram is displayed in Fig. 9. When the transducer is operating in the classical pulse mode, the bottom of the hole is clearly visible. The absence of a sharp discontinuity on the upper horizontal

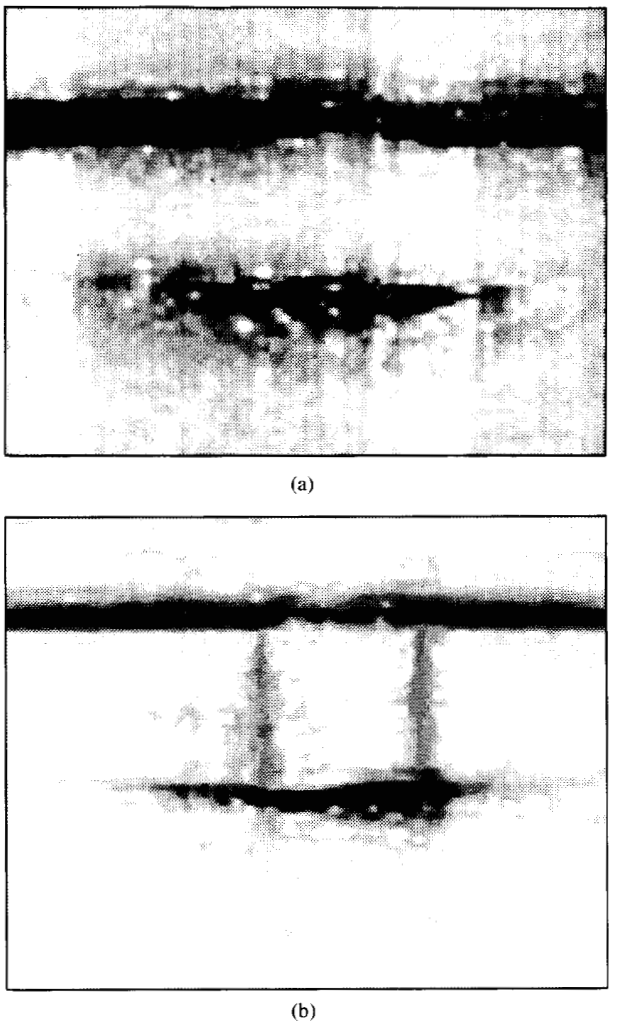

Fig. 9. Echo B type image of a single hole drilled in AGA14 (dural). (a) Pulse method. The bottom of the hole is clearly visible. (b) Correlation with m-sequence. The bottom and the side walls of the hole are visible. Hole dimensions: diameter = 3 mm, depth = 10 mm.

line of echogram indicates a beam width on the order of the diameter of the hole.

It should be pointed out that when m-sequences are used, the walls of the drilled hole are clearly visible. At this stage we do not have a clear explanation of the effect, but we suspect that it could be due to mode conversion in the sample. As suggested by one of the referees, "it could be because the receiver annuli is at an angle relative to the wall or it may be just the effect of the top edge of the wall elongating the pulse." This effect, never seen in classical echography, is clearly visible in correlation techniques because the local dynamic range is improved by band compression.

VII. Conclusion

Since the mid-1980's it has been accepted that "Golay code correlation systems provide as good as or better performance than an m-sequence (noncircular) correlation system."

In this paper we have used a circular m-sequence correlation system. Since in this case the coded signal is emitted continuously, the system needs at least two transducers operating in emission and reception mode, respectively. In our opinion

multielement transducers such as the one that we used in this study are no longer a technical problem. Furthermore, it has its own advantages, since it could provide focus tracking and electronic apodization of the ultrasonic beam. Simulation of the ambiguity function has shown that m-sequence circular correlation provides the same order of magnitude of secondary lobes as Golay codes.

For a metallic reflector immersed in a water tank the SNR observed with m-sequences is 20 dB higher than the SNR observed with Golay complementary series. It was shown that the modulation-demodulation scheme leads to the observed SNR degradation. Direct sequencing could probably improve the value of SNR and we shall evaluate its merits in the near future. We have demonstrated however that even if in perfectly stationary media, Golay series could be advantageous. This seems no longer be correct when the medium is in motion.

Finally, we wish point out that in spite of numerous A type echograms available in the literature there are only a few 2-D (B type) images [8], [9], [41].

We hope that the results presented in this paper will develop greater interest in the use of coded signals in ultrasonic echography. Imaging objects with less dramatic changes in acoustical impedance will be our next area of investigation.

ACKNOWLEDGMENT

It is a pleasure to thank Dr. P. C. Kahn for a critical reading of the manuscript and the referees for their constructive remarks.

REFERENCES

[1] M. M. Bilgutary, E. S. Furgason, and V. L. Newhouse "Evaluation of random signal correlation for ultrasonic flaw detection," *IEEE Trans. Sonics Ultrason.*, vol. SU 23, no. 5, pp. 329–333, 1976.

[2] M. Gindre, C. Lebeault, F. Rieuneau, W. Urbach, and J. Perrin, "Ultrasonic imaging using correlation techniques: Computer simulations and experimental results," in *Acoustical Imaging.* New York: Plenum, 1988, vol. 17.

[3] J. Max, "Méthodes et techniques de traitement du signal et applications aux mesures physiques," vol. 1, Masson, Ed., Paris, France, 1987.

[4] C. Elias, "An ultrasonic pseudorandom signal correlation system," *IEEE Trans. Sonics Ultrason.*, vol. SU 27, no. 1, pp. 1–7, 1980.

[5] F. Lam and M. Hui, "An ultrasonic pulse compression system using maximal length sequences," *Ultrason.*, vol. 20, no. 3, pp. 107–112, 1982.

[6] M. Gindre, "Conception et réalisation d'un échographe à corrélation," Ph.D. dissertation, Univ. of Paris V, 1987.

[7] H. Bressmer, V. Heinze, and U. Faust, "Verbesserung der qualität von ultraschall B-bildaufnahmen durch anwendung der pulskompression-sme\ss ₸echnik," Biomedizinische Technik Band, 35, Ergänzungsband, pp. 274–275, 1990.

[8] H. Bressmer, P. Kugel, and U. Faust, "Pulse compression—A very good method to improve the quality of B-Modes images," 1st Euro. Conf. Biomed. Eng., Nice, France, 1991.

[9] M. O'Donnell, "Coded excitation system for improving penetration of real time phased array imaging systems," *IEEE Trans. Ultrason., Ferroelec., Freq. Contr.*, vol. 39, pp. 341–351, 1992.

[10] B. B. Lee and E. S. Furgason, "High speed digital Golay code flaw detection system," *Ultrason.*, vol. 21, pp. 153–161, 1983.

[11] G. Hayward and Y. Gorfu, "A digital hardware correlation system for fast ultrasonic data acquisition in peak power limited applications," *IEEE Trans. Ultrason., Ferroelec., Freq. Contr.*, vol. 35, no. 6, pp. 800–808, 1988.

[12] W. H. Chen and J. L. Deng, "Ultrasonic non destructive testing using Barker code pulse compression techniques," *Ultrason.*, vol. 26, pp. 23–26, 1987.

[13] G. S. Kino, *Acoustic waves: devices, imaging, and analog signal processing.* Englewood Cliffs, NJ: Prentice-Hall, 1987, p. 390.

[14] M. Bernfeld and P. M. Liebman, "On a property of binary sequences," *Proc. IEEE*, vol. 52, p. 744, 1964.

[15] R. H. Barker, "Group synchronisation of binary digital systems," in *Communications Theory.* New York: Academic, 1958.

[16] S. W. Golomb and R. A. Scholtz, "Generalized Barker sequences," *IEEE Trans. Inform. Theory*, vol. IT-11, no. 4, pp. 533–537, 1965.

[17] E. E. Hollis, "Comparison of combined Barker codes for Radar use," *IEEE Trans. Aerospace and Electron. Syst.*, vol. AES-3, no. 1, pp. 141–144, 1967.

[18] S. W. Golomb, *Digital Communications with Space Applications.* Englewood Cliffs, NJ: Prentice Hall, 1964.

[19] D. V. Sarwate and M. B. Pursdey, "Crosscorrelation properties of pseudorandom and related sequences," *Proc. IEEE*, pp. 593–619, 1980.

[20] M. J. Golay, "Complementary series," *IRE Tans. Inform. Theory*, vol. IT-7, pp. 82–87, April 1961.

[21] E. E. Hollis, "A property of decomposable Golay codes which greatly simplifies sidelobe calculation," *Proc. IEEE*, pp. 1727–1728, 1975.

[22] ——, "Another type of complementary sequences," *IEEE Trans. Aerospace and Electron. Syst.*, vol. AES-11, no. 5, pp. 916–920, 1975.

[23] R. Turyn, "On Barker codes of even length," *Proc. IEEE*, vol. 51, p. 1256, Sept. 1963.

[24] R. L. Frank, "Polyphase codes with good nonperiodic correlation properties," *IEEE Trans. Inform. Theory*, vol. IT-9, no. 1, pp. 43–45, 1963.

[25] C. E. Cook and M. Bernfeld, *Radar signals, An introduction to theory and applications.* New York: Academic, 1967.

[26] D. A. Huffman, "The generation of impulse equivalent pulse trains," *IRE Trans. Inform. Theory*, vol. IT-8, pp. 10–16, 1962.

[27] M. H. Ackroyd, "The design of Huffman sequences," *IEEE Trans. Aerospace and Electron. Syst.*, vol. AES-6, pp. 790–796, 1970.

[28] ——, "Synthesis of efficient Huffman sequences," *IEEE Trans. Aerospace and Electron. Syst.*, vol. AES-8, no. 1, pp. 2–8, 1970.

[29] F. F. Kretschmer and Lin, "Huffman coded pulse compression waveforms," RNL Rep. 8894, Naval Res. Lab., Wash., DC, pp. 94–108, Feb. 1985.

[30] F. de Coulon, *Théorie et traitement des signaux.* Paris, France: Dunod, 1987.

[31] B. B. Lee and E. S. Furgason, "The use of correlation systems for real time ultrasonic imaging," in *Proc. IEEE Ultrason. Symp.*, 1985, pp. 782–787.

[32] Y. Takeuchi, *Comparison of apodized linear FM chirp and complementary series.* Hino: Yokogawa Medical Systems, Ltd., 1981.

[33] R. Kuc, "Generating a minimum-phase digital filter model for the acoustic attenuation of soft tissue," *IEEE Ultrason. Symp.*, 1983.

[34] F. Roddier, *Distributions et transformations de Fourier.* New York: McGraw Hill, 1978.

[35] M. Fink, J-F. Cardoso, and P. Laugier, "Analyse des effets de la diffraction en échographie médicale," *Acta Electronica*, vol. 26, no. 1-2, pp. 59–80, 1984.

[36] M. Labarrere, J. P. Krief, and B. Gimonet, *Le filtrage et ses applications.* Toulouse, France: Cépadues, 1982.

[37] A. Oppenheim and R. Schafer, *Digital signal processing.* Englewood Cliffs, NJ: Prentice-Hall, 1975.

[38] J. Liferman, *Les techniques rapides de traitement du signal: Fourier, Walsh, Hadamard.* Paris, France: Masson, 1979.

[39] P. M. Morse and K. U. Ingard, *Theoretical acoustics.* Princeton, NJ: Princeton Univ. Press, 1968.

[40] B. B. Lee and E. S. Furgason, "An evaluation of ultrasound NDE correlation flaw detection systems," *IEEE Trans. Sonics Ultrason.*, vol. SU-29, no. 6, pp. 359–369, 1982.

[41] G. Hayward and Y. Gorfu, "Low power ultrasonic imaging using digital correlation," *Ultrason.*, vol. 27, no. 5, pp. 288–296, 1989.

Mohamed A. Benkhelifa was born in Mostaganem, Algeria, on July 10, 1965. He received the degree in electronic engineering from the U.S.T.O. (Oran-Algeria) in 1987. He received the D.E.A. in instrumentation, from the University of Orsay, Paris Sud in 1992. The title of his thesis was "Echography using correlation techniques: choice of coding signal."

He now teaches at Cergy University, Department of Electrical Engineering and Computer Science. His research interests include signal processing in echography.

Marcel Gindre (M'89) received the electronics engineer degree from CNAM Paris in 1971, the Diplome de Docteur Ingénieur from the Orsay University (Paris XI) and the Docteur és sciences degree in Physics from University of Paris V in 1987.

He is Professor of electronics at the Institut of Technology of Cergy Pontoise University France. His current research interests include signal processing, numeric simulation, and electronic circuits in ultrasonic applications.

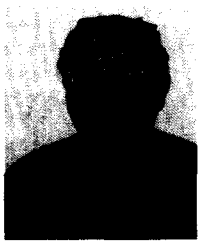

Jean-Yves Le Huérou received the electronics engineer degree from the Conservatoire National des Arts et Métiers (CNAM) Paris, France, the DEA degree in 1989, and the Diplome de doctorat en sciences physiques de l'Université Paris V in 1993.

Since 1989 he has been with the Laboratoire d'Imagerie Paramétrique Paris, France. His research fields include acoustical transducer electronics and digital signal processing techniques in ultrasonic imaging. He also teaches electronics at Cergy Pontoise University France.

Wladimir Urbach, photograph and biography not available at the time of publication.